ELSEVIER

Microelectronics Journal 33 (2002) 495–500

Microelectronics Journal

www.elsevier.com/locate/mejo

Gate controlled 2-DEG varactor for VCO applications in microwave circuits

A. Anwar[a], B. Nabet[a], R. Ragi[b], J.E. Manzoli[c], M.A. Romero[b,*]

[a]*Department of Electrical and Computer Engineering, Drexel University, Philadelphia, PA 19104, USA*
[b]*Department of Electrical Engineering, University of São Paulo, Ave. Dr. Carlos Botelho 1465 São Carlos, SP 13564-250, Brazil*
[c]*Nuclear Energy Research Institute, IPEN-CNEN, São Paulo, SP, Brazil*

Received 24 April 2001; revised 27 August 2001; accepted 21 September 2001

Abstract

A novel gate controlled Schottky diode varactor is introduced. The three-terminal varactor is a modulation-doped heterostructure of AlGaAs/GaAs with two Schottky contacts, similar to a metal–semiconductor–metal (MSM) diode. Schottky metal contacts are made to a two-dimensional electron gas (2-DEG). The third contact, the gate contact is formed from highly doped n^+ GaAs material to allow an open optical window that can be used for optical gating and mixing. Structure capacitance is less than 1 PF and a change of more than 30% from the zero bias capacitance is observed with the applied gate voltage. On the basis of our quasi two-dimensional C–V model, the layer structure and device dimensions can be optimized and scaled to cover a wide range of operations in the microwave and millimeter wave regimes.

Keywords: Varactor; Voltage controlled oscillator; Optically controlled oscillator; Two-dimensional gas; Mixing

1. Introduction

Varactors have extensive applications in communication transceivers and control systems circuitry. They are the main building blocks in voltage controlled oscillators (VCOs). Schottky diode varactors were vastly investigated for frequency multiplication applications. These devices have a symmetric C–V characteristics as well as asymmetric I–V characteristics. This makes them good candidates for generation of odd harmonics with high efficiency [1,2]. Also, due to lack of charge storage time delays, Schottky diodes have the added advantage of high-speed operation compared to PIN diodes. Their most important property, however, is that Schottky contacts are routinely deposited as gates of MESFETs, making these devices compatible with unipolar MMIC technology. The comparison of PIN and HBT combinations would be the natural choices in bipolar technology. Varactors as variable capacitance devices, they utilize the voltage dependence of semiconductor junction capacitance. Generally, for any semiconductor junction with arbitrary doping profile $N = Bx^m$, the capacitance equals

$$C = \frac{\partial Q}{\partial V} = \left[\frac{qB(\varepsilon_o \varepsilon_r)^{m+1}}{(m+2)(V + V_{bi})} \right]^{1/(m+2)} \quad (1)$$

Eq. (1) shows that the capacitance varies with the reverse terminal applied bias as $C \propto (V + V_{bi})^{-s}$, with sensitivity $s = (m + 2)^{-1}$. For a uniformly doped abrupt junction this reduces to the usual inverse square root bias dependence for the capacitance. In Schottky diode varactors the junction capacitance changes, as the reverse applied bias voltage depletes the semiconductor channel until it reaches its minimum geometrical capacitance. Although some variations due to the charge storage can still be observed, further increase on the applied bias typically causes no significant effect.

With the advent of modulation doped devices such as MODFETs, with their improved transconductance, high bandwidth and high noise margins, development of other devices that take advantage of transport in reduced dimensional regimes becomes important. To that end Schottky diodes in which contact is made to a two-dimensional electron gas (2-DEG) were realized [3,4]. These devices take advantage of the 2-DEG characteristics and produce a lower series resistance while, due to streamlines of the

* Corresponding author. Tel.: +55-16-273-9349; fax: +55-16-273-9372.
E-mail address: muriloa@sel.eesc.sc.usp.br (M.A. Romero).

0026-2692/02/$ - see front matter © 2002 Elsevier Science Ltd. All rights reserved.
PII: S0026-2692(01)00142-2

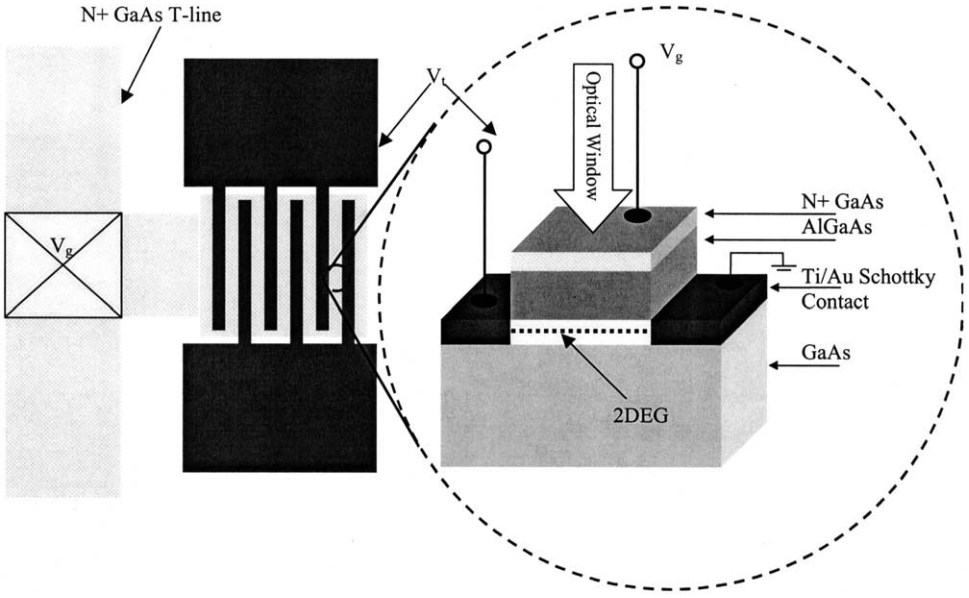

Fig. 1. Structure of the 2DEG varactor showing terminal contacts and the n^+ transparent gate.

electric field between 2-DEG and 3-D metal; they achieve wider depletion region and higher breakdown voltage. They were shown to be efficient frequency triplers in the millimeter and sub-millimeter ranges [5,6]. Up to now we are unaware of any comprehensive theoretical description of the $C-V$ characteristics for such structures. In any case, it was theoretically expected that the depletion width of the ideal junction between metal to 2-DEG is linearly dependent on the voltage [7,8] and hence capacitance should show a stronger voltage dependence compared with metal to bulk contact.

In what follows we propose what is, to our knowledge, the first theoretical model of the $C-V$ characteristics of a device in which two back to back Schottky contacts are made to a 2-DEG channel formed through modulation doping of a heterostructure. While maintaining desirable properties of the 2-DEG Schottky diode, this heterojunction metal–semiconductor–metal (HMSM) device has the advantage of ease of fabrication, since both contacts are deposited on the same step. The structure is implemented and experimental results are presented. An important distinguishing feature of the novel device proposed here is the addition of a third contact, gate, that allows a second degree of freedom to modulate the capacitance, in particular, and channel characteristics, in general. Since the major potential application of the HMSM device is in optical detection [9], we chose to fabricate the gate for this varactor HMSM by using a thin layer of highly doped n^+ material. This layer is mostly transparent to light hence the device can be optically gated to achieve a third degree of freedom that is very useful for optical mixing applications.

Three-terminal varactors previously investigated have used the gate-to-source capacitance of the GaAs MESFET [10–12] device using the drain contact as the third terminal. As compared to the device proposed here, the two main advantages are transport in reduced dimensional regime and the light transparency of the gate.

2. Device description and experimental results

The structure of the HMSM-varactor is shown in Fig. 1. On top of a buffer layer grown on semi-insulating GaAs substrate, 5000 Å of undoped GaAs was deposited, followed by 100 Å of undoped $Al_{24}Ga_{76}As$ and 500 Å of $3\times10^{17}\,cm^{-3}$ n-type $Al_{24}Ga_{76}As$. The topmost layer is 200 Å of $3\times10^{18}\,cm^{-3}$ n-type GaAs layer. All growth was done by molecular beam epitaxy (MBE) and the structure was chosen to be compatible with enhancement type MODFETs where the n^+ cap layer is usually used for ohmic contact formation. A trench was formed by wet chemicals etching through the $Al_{24}Ga_{76}$ As layers and 500 Å of Schottky Ti/Au contact metal was deposited on the GaAs side to form Schottky junctions with the 2-DEG. The contacts have the usual interdigital structure. Since the cathode and anode terminals are recessed, the top n^+ layer readily becomes available for probing and voltage application. For better electrical access, however, a third metal contact may be deposited on the n^+ layer, away from the interdigital surface. The use of the n^+ layer as transparent electrode was previously demonstrated in photodetectors, where large increase in responsivity due to better optical coupling was reported [13].

The capacitance–voltage characteristics of the device were measured by directly probing the three-terminals and recording the results by a HP LCR meter. Fig. 2 shows the measured capacitance as a function of terminal voltage for two voltages applied to the gate. It is seen that a large

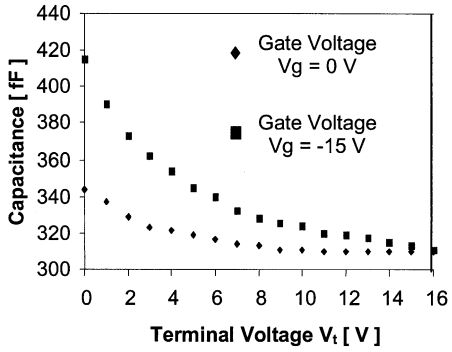

Fig. 2. Variation of terminal capacitance with terminal voltage for two gate voltages.

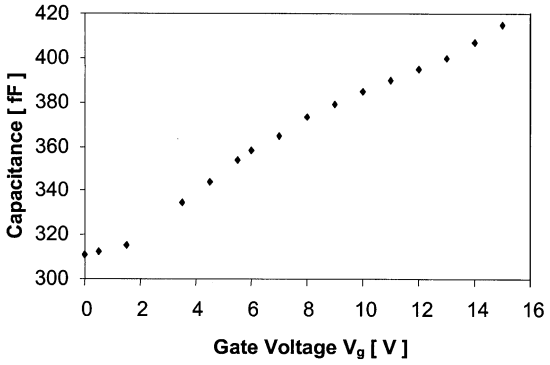

Fig. 3. Modulation of terminal capacitance with gate voltage at zero terminal voltage.

variation (about 24%) of capacitance can be obtained when a signal of −15 V is applied to the gate terminal. Defining sensitivity of a varactor as the difference between capacitance at zero bias and its minimum geometrical limit, it is seen that the gate signal substantially extends the sensitivity.

Independent of the physical mechanism responsible for charge modulation by the applied bias, if the voltage is high enough to fully deplete the semiconductor, the capacitance between the electrodes will reach a strictly geometrical lower value given by [14]

$$C_G = L(N-1)\varepsilon_0(\varepsilon_r+1)\frac{K(k)}{K(k')} \tag{2}$$

where ε_r is the relative dieletric constant of the semiconductor, ε_0 is the dieletric permittivity in vacuum, K is the elliptic integral of the first kind, N is the number of electrodes, L is the electrode length and

$$k = \cos\left(\frac{\pi}{2}\left(1-\frac{W}{W+G}\right)\right)$$

is a dimensionless quantity, where W is the electrode width and G is the electrode fingers spacing. This same minimum value was reached when the n^+ and AlGaAs layers were etched. In that case, the zero bias capacitance was slightly higher than the minimum value indicating that most of the bulk material between electrodes was already depleted. In fact, modulation doping reduces this depletion region by virtue of the existence of 2-DEG carriers; the gate simply modulates the sheet carrier density and hence changes the capacitance. It should be mentioned that an important attribute of this device is that the terminal current is very low and was always maintained under 10 nA for a $200\times200\ \mu m^2$ device. Previous three-terminal varactors that used MESFET devices need currents in mA range for their operation [10–12]

In Fig. 3 capacitance is plotted as a function of gate voltage for zero terminal bias voltage. It is seen that capacitance changes from 311 to 417 fF, a change of about 35% for a gate voltage variation of 15 V. It is observed that a large gate voltage is needed to achieve capacitance modulation. This can be related to the voltage drop along the n^+ layer lines, which, although highly doped, is very thin and has a long length. One way to enhance the device sensitivity to gate voltage is to sacrifice its fabrication simplicity by aligning and depositing gate metal. This solution, however, in addition to requiring more processing effort, would suppress the optical coupling capability.

3. Theoretical modeling

The model presented in this section is a quasi two-dimensional extension of a work previously published by the authors [15]. Here, we start by self-consistently solving Schrödinger and Poisson equations in the growth direction. The quantum-mechanical formalism is based on the effective mass approximation, where the electron wavefunction is taken as the product of a Bloch function and an envelope function, solution of the time-independent Schrödinger equation:

$$H\phi_i(x) = E_i\phi_i(x) \tag{3}$$

The utilized Hamiltonian takes into account position-dependent effective mass and lattice constant and is given by [15]

$$H = -\frac{\hbar^2}{2a(x)}\frac{d}{dx}\frac{[a(x)]^2}{m^*(x)}\frac{d}{dx}\frac{1}{a(x)} + V_{ef}(x) \tag{4}$$

where x is taken as the direction perpendicular to the epitaxial layers. The effective potential V_{ef} is given as the sum of four terms

$$V_{ef}(x) = V_e(x) + C_1(\varepsilon_{xx}+\varepsilon_{yy}+\varepsilon_{zz}) + V_H(x) + V_{xc}(x) \tag{5}$$

where V_e represents the conduction-band edge potential of the undoped structure, i.e., the band-diagram discontinuities and V_H is the Hartree term due to the electrostatic potential. For completeness, we have also included an exchange-correlation term, V_{xc} while the strain caused by lattice mismatch due, for example, to the insertion of an InGaAs pseudomorphic channel layer in between the AlGaAs/GaAs heterojunction can be accounted for the second term of the RHS of Eq. (5). In this term, C_1 is the conduction band

deformation potential and ε_{xx}, ε_{yy} and ε_{zz} are the strain components [15].

The Poisson equation, which yields the above mentioned Hartree term, is given by

$$\frac{\mathrm{d}}{\mathrm{d}x}\left(\varepsilon_o\varepsilon_r(x)\frac{\mathrm{d}}{\mathrm{d}x}\right)V_H(x) = -q[N_D^+(x) - N_A^- - n(x)] \tag{6}$$

where q is the electronic charge, $\varepsilon_r(x)$ is the position dependent dielectric constant of the semiconductor, N_D^+ is the ionized donor concentration, N_A^- is the ionized non-intentional background acceptor concentration and $n(x)$ is the free-electron concentration in the conduction band (the free hole concentration was neglected). We write $n(x)$, in terms of the electronic eigenfunction $\phi_i(x)$, as

$$n(x) = \frac{m_o^* kT}{\pi\hbar^2}\sum_i \ln\left[1 + \exp\left(\frac{E_f - E_i}{kT}\right)\right]|\phi_i(x)|^2 \tag{7}$$

where m_o^* is the electron effective mass in the 2-DEG channel, k is the Boltzmann constant, T is the absolute temperature, h is the reduced Planck constant, E_f is the Fermi level energy and E_i represents the ith eigenvalue. Summation is carried out over all i subbands.

The ionized donor concentration N_D^+ is described by

$$N_D^+(x) = \frac{N_D(x)}{1 + g_n\exp[(E_f - E_d)/kT]} \tag{8}$$

where N_D is the position dependent donor concentration, g_n is the donor level spin degeneracy factor, taken as equal to 2, and $E2_D$ is donor ionization energy.

The Fermi-level position E_f is computed from the usual charge neutrality condition in the bulk material and the above formulation (Eqs. (3)–(8)) must be solved self-consistently in real space. In particular, the eigenstates of the Schrödinger equation are numerically calculated by using a split-operator algorithm through a non-uniform finite difference discretization scheme [15], under the boundary conditions that the wavefunction must vanish at the substrate and at the Schottky barrier. The boundary conditions for the Poisson equation are given by the applied gate voltage V_g at the Schottky barrier (taken as $x = 0$) as well as by the position of the conduction band with respect to the Fermi-level in the bulk semiconductor, presenting a non-intentional background ionized doping density N_A^-. The solution yields the charge control relation between the gate voltage V_g and the sheet electron density n_s into the channel, i.e. $n_s = f(V_g)$ [16,17]. Now, this charge control relation is used as an input to develop the first quasi two-dimensional for the capacitance–voltage characteristics of 'gated' HMSM devices (see Fig. 1). The y-component of the potential distribution along the channel, $V(y)$, is taken into account by, as usually done [16,17] in the modeling of other 2-DEG based devices, assuming that if $n_s = f(V_g)$ one can write $n_s(y) = f(V_g - V(y))$, preserving the same functional dependence $f(.)$.

Accordingly, in our procedure, for a given terminal voltage, the channel is initially divided into several segments of length dy. Next, the capacitance contribution of each segment is computed by solving the one-dimensional Schrodinger–Poisson problem in the growth direction (Eqs. (3)–(8)), but now under an effective gate potential $V'_g = V_g - V(y_i)$, where y_i is a coordinate position located in the middle of each segment. A quasi-static approach was used, yielding the capacitance per unit area as the total charge variation caused by a small voltage change around a given bias point.

Then, this free-carrier capacitance, C_{free}, is given by the summation of the capacitance contribution for each segment dy. The overall device capacitance is finally written as

$$C_T = C_{free} + C_G \tag{9}$$

where C_G is the geometry-related component, given by Eq. (2).

The model is expected to provide reliable results as long as an accurate expression for $V(y)$ is used (see, for example, Ref. [8]) and the length of each segment dy is small enough. Fig. 4 displays the free-carrier capacitance contribution (see Eq. (9)) as a function of the terminal voltage for a hetero-dimensional Schottky–Ohmic device, without a gate contact. The simulated presents the same layer structure as the fabricated varactors discussed in the previous section and a total area of 40 μm × 40 μm. Since there is no gate present, in the simulations V_g was replaced by a surface potential of 0.75 V, due to surface states at the AlGaAs/air interface.

The theoretical results obtained are quite promising. It is clearly seen that our model was able to reproduce, without any fitting parameter, the general features of the varactor C–V characteristics, yielding capacitance values in the measured range. Given the uncertainty on some device parameters (such as the amount of non-intentional doping at the GaAs buffer layer and the value of the surface potential at the top of the structure) no attempt will be made in this paper to directly match theory and experiment. However, due to satisfactory results obtained above, we believe that this novel model will be a powerful tool to optimize the device performance, by providing useful design guidelines. Further results will be presented elsewhere.

4. Conclusions

A novel gate-controlled varactor was realized. The device takes advantage of Schottky contact to a 2-DEG, which is produced by modulation doping of an AlGaAs/GaAs heterojunction. The gate is formed from an n^+ cap layer that is normally used for ohmic contact deposition. Therefore, device growth architecture is the same as used in MODFETs.

The gated device extends the sensitivity of a comparable device fabricated without the gate by about 24% while the zero bias capacitance can be changed by 35% for a gate

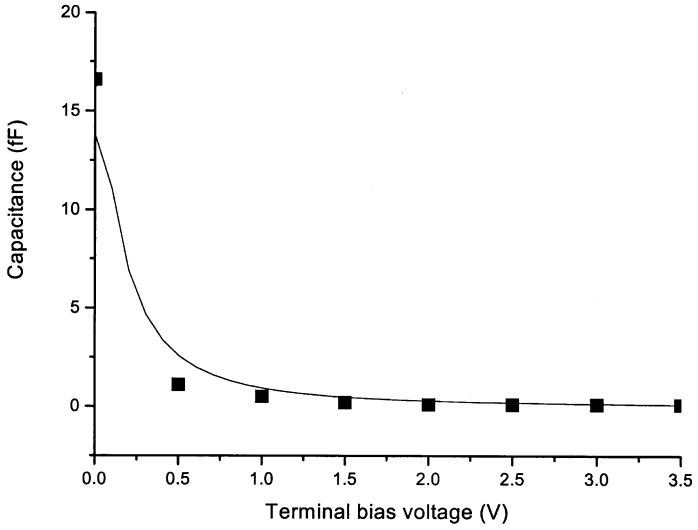

Fig. 4. Free-carrier contribution for the capacitance for a Schottky–Ohmic heterodimensional device. The solid line is the theoretical result while the squares represent experimental data. The figure does not includes the capacitance component described by Eq. (2). For the geometric contribution Ref. [14] yields 23.6 fF although a value of 2 fF was measured.

voltage variation of 15 V. This adds a degree of controllability to reach the DC free running oscillator frequency design goal, especially useful in a low yield MMIC process. Another application of this device is its operation as a mixer because the capacitance and thus the oscillating frequency are both a function of the terminal and the gate voltages V_t and V_g, respectively, i.e., $C = f(V_t, V_g)$. This means that frequency can be modulated by a mixed signal from gate and junction terminals. A further application of the device is the one where the varactor is in parallel with an active device and the variation of the terminal voltage affects the operating point of the active network. The varactor gate can be utilized to modulate the junction capacitance without introducing added bulky isolation circuits. Also, another important feature of the varactor is the optical transparency of the gate. This allows for optical gating of the varactor and makes it a good candidate as an optically controlled oscillator (OCO). Finally, since carrier transport along the two terminals is determined by Schottky-2-DEG contact, current conduction remains under 10 nA for a relatively large size device. Hence, power consumption remains minimal and the device behaves quite favorably compared to MODFET based OCO's [5]. Finally the use of the quasi two-dimensional $C–V$ model presented in this paper will allow further enhancement of the varactor performance.

Acknowledgements

This work was supported in part by NSF (National Science Foundation) through award no. DUE 6950350, Fapesp-São Paulo State Research Foundation under grants no. 96/11290-2 and 97/01591/8 and Motorola do Brasil.

References

[1] S.M. Nilsen, H. Gronqvist, H. Hjelmgren, A. Rydgerg, E.L. Kollberg, Single barrier varactors for submillimeter-wave power generation, IEEE Transactions on Microwave Theory and Techniques 41 (4) (1994) 572–579.

[2] J.T. Louhi, A.V. Raisanen, N.R. Erickson, Cooled Schottky varactor frequency multiplier at submillimeter wavelengths, IEEE Transactions on Microwave Theory and Techniques 41 (4) (1994) 565–5571.

[3] W. Peatman, M. Shur, H. Park, T. Yetterdal, R. Tsai, M. Hurt, Narrow channel 2-D MESFET for low power electronics, IEEE Transactions on Electron Devices 42 (9) (1995) 1569–1573.

[4] B. Nabet, A Heterojunction Metal–Semiconductor–Metal Photodetector, IEEE Photonics Technology Letters 9 (2) (1997) 223–225.

[5] W.C. Peatman, T.W. Crowe, M. Shur, A novel Schottky/2-DEG diode for millimeter- and submillimeter-wave multiplier applications, IEEE Electron Device Letters 13 (1) (1992) 11–13.

[6] P.J. Koh, W.C. Peatman, T.W. Crowe, Millimeter wave tripler evaluation of a metal/2-DEG Schottky diode varactor, IEEE Microwave and Guided Wave Letters 5 (2) (1995) 73–75.

[7] B.L. Gelmont, W. Peatman, M. Shur, Heterodimensional Schottky metal–two-dimensional electron gas interface, Journal of Vaccum Science and Technology B11 (14) (1993) 1670–1674.

[8] S.G. Petrosyan, A.Y. Shik, Contact phenomena in a two-dimensional electron gas, Sov. Phys. Semic. 23 (1989) 696–697.

[9] F. Castro, B. Nabet, A. Anwar, Schottky contact between metal and two-dimensional electron gas: device applications to low-noise optical detectors, Proceedings of SBMO/IEEE MTT-S International Microwave and Optoelectronics Conference, Natal, Brazil, August 11–14, 1997, pp. 323–326.

[10] S. Xiaowei, L. Jinsheng, Z. Zongming, C. Jinrong, L. Jinting, A MESFET variable-capacitance model for realizing MMIC voltage-controlled function, Microwave and Optical Technology Letters 12 (1) (1996) 31–33.

[11] J.Y. Lee, C.J. Lee, U.S. Hong, A novel design of voltage controlled dielectric resonator oscillator using 3-terminal MESFET varactor, Journal of the Korean Institute of Telematics and Electronics 30A (12) (1993) 28–35.

[12] J. Lin, T. Itoh, Tunable active bandpass filters using three-terminal MESFET varactors, 1982 IEEE MTT-S International Microwave Symposium Digest, New York, NY, USA, pp. 921–924.
[13] R.B. Darling, B. Nabet, J.E. Samaras, S. Ray, E.L. Carter, Epitaxial n^+ layer GaAs Mesa-Finger interdigital surface photodetectors, IEEE Electron Device Letters 10 (10) (1989) 461–463.
[14] H. Engan, Excitation of elastic surface waves by spatial harmonics of interdigital transducers, IEEE Transactions on Electron Devices 16 (12) (1969) 1014–1017.
[15] J.E. Manzoli, M.A. Romero, O. Hipólito, On the capacitance–voltage modeling of strained quantum-well MODFETs, IEEE Journal of Quantum Electronics 34 (12) (1998) 2314–2320.
[16] K. Lee, M.S. Shur, T.J. Drummond, H. Morkoç, Current–voltage and capacitance–voltage characteristics of modulation-doped field-effect transistors, IEEE Transactions on Electron Devices 30 (3) (1983) 207–212.
[17] H. Rohdin, P. Roblin, A MODFET DC model with improved Pinchoff and saturation characteristics, IEEE Transactions on Electron Devices 33 (5) (1986) 664–672.